ACS OMEGA

Article

Cite This: ACS Omega 2018, 3, 5399−5405

# Rapid Induction and Microwave Heat-Up Syntheses of CdSe Quantum Dots

Hongfu Luo, Bemnet A. Kebede, Emily J. McLaurin,* and Viktor Chikan*

Department of Chemistry, Kansas State University, 213 CBC Building, 1212 Mid-Campus Dr North, Manhattan, Kansas 66506-0401, United States

Supporting Information

**ABSTRACT:** The production of nanoparticles on an industrial scale requires an approach other than the widely used hot-injection method. In this work, two heat-up methods are applied to nanoparticle synthesis. The induction heating method produces CdSe quantum dots with ultrasmall properties in seconds. Initial flow-through experiments demonstrate that induction heating continuously produces quantum dots. These results are compared with those from microwave synthesis, which produces quantum dots on a longer timescale but provides fast, continuous heating. Both methods can produce quantum dots within seconds because of rapid heating. In addition, different precursors, single source and separate source, give different results, ultimately providing a handle to control quantum dot properties.

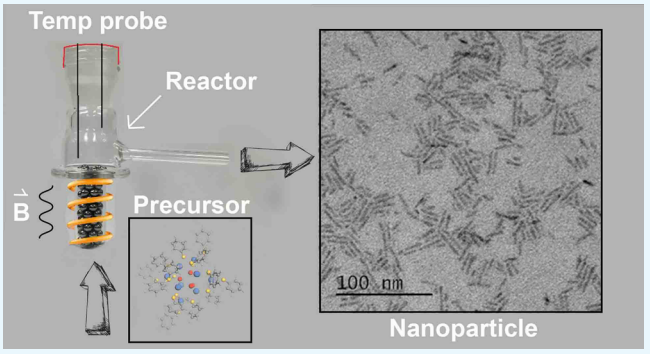


## INTRODUCTION

Semiconducting nanoparticles have a variety of unique properties that are different from those of their bulk counterparts because of quantum confinement and their large surface-to-volume ratios. These properties inspire interest in applications such as solar cells,[1−3] batteries, bioimaging,[4,5] catalysis,[6−9] and data storage.[10] The strong dependence of these properties on their diameter means that controlling the size of these particles is crucial to tuning these characteristics.[11] CdSe quantum dots (QDs) have been studied extensively as a model system of such particles. The ability to manufacture QDs on a large scale is of critical interest because low-cost fabrication methods are a large advantage of these materials. It is important to produce highly homogeneous, monodispersed QDs in a bench-top synthesis route with potential for scale-up production and control over their surface chemistry, crystalline structure, and shape.[11]

Heat-up methods for QD synthesis are well-established but significantly less popular than hot-injection methods.[12] Most methods employ rapid-heating techniques to achieve narrow size distributions by separation of particle nucleation and growth.[13,14] Methods analogous to hot injection often suffer from unoptimized conditions and reliance on established procedures. The most general method is a simple combination of precursors used in hot injection in a flask followed by heating up the flask using an external heat source such as an oil bath or a heating mantle. The high temperatures used for formation of high-quality QDs often take minutes to attain (Figure 1a). An alternative is microwave (MW)-assisted heating, in which MWs applied to the reaction mixture can rapidly increase temperature (Figure 1b).[15] Here, we demonstrate the use of a new method, induction heating (IH), to synthesize QDs in a batch and flow reactor. Although IH has been used for chemical synthesis,[16] it has not been used for QD synthesis, to the best of our knowledge.

IH uses eddy currents generated in a conductor by applying a rapidly alternating magnetic field, usually produced by an electromagnet. The heat generated in the material through Joule heating is proportional to the resistance of the conductor. In addition, ferromagnetic materials can produce heat more efficiently in the presence of alternating magnetic fields because of the movement of magnetic domain walls. The increased temperature of the conductor results in an increased resistance, which increases the amount of heat generated, forming a positive feedback loop where the heating rate increases with time. In comparison, the heat generated by MW heating is result of a combination of dipolar rotation and ionic conduction.[17] Heat generated by ionic conduction is linear with respect to time. Because of the different characteristics and mechanisms of the two heating methods, it increases the number of collisions, further increasing the heating rate, but heating from dipolar rotation generally decreases at higher temperatures. MW heating is valued for heat-up QD synthesis because of rapid heating rates.[18,19] It is reasonable to expect IH to be an interesting method for QD syntheses for its extremely high heating rate. Rapid heating is critical in the separation of

Received: January 16, 2018
Accepted: April 23, 2018
Published: May 21, 2018






DOI: 10.1021/acsomega.8b00096
ACS Omega 2018, 3, 5399−5405

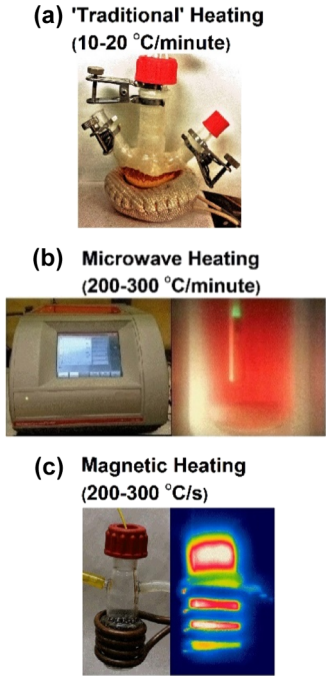


**Figure 1.** Pictures of the experimental setups used in this work: (a) heating mantle, (b) MW reactor and a camera image, and (c) IH and a thermal camera image.

nucleation and growth rates of QDs in homogeneous colloidal solutions.[14] This study demonstrates that the rapid heating rates from IH can shorten the nucleation stages during QD growth and provide greater control of particle size and size distribution. Comparison of the results with those from MW heating shows that the MW method also has its unique advantages such as rapid, uniform, controlled heating.

## RESULTS AND DISCUSSION

In nanoparticle synthesis, the rate of heating affects the nucleation and growth rates with important consequences for the final size and size distribution of the particles. With the experimental setup as shown in top of Figure 1, IH routinely achieved a heating rate of 110 °C/s,[20] whereas a conventional heating mantle heats at 1 °C/s. Dodecylamine (DDA) is chosen as a solvent for its ability to stabilize the QD product at room temperature in a solid-phase matrix. To prevent unintended decomposition, the precursor complex $Li_4[Cd_{10}Se_4(SPh)_{16}]$ is slowly dissolved in DDA in a water bath while being well-stirred so that no part of the reaction mixture is exposed to temperatures higher than 70 °C. To prevent oxidization during synthesis and cooling, the solution mixture is purged under argon after being loaded into the reaction vessel through two needles injected on the top for 5 min. The heating rate is controlled by the induction current. The temperature rise can be measured with a fiber optic temperature probe, and it also can be estimated from the boiling of degassed solvents. Estimation from the boiling point of the solvents puts the heating rate at 200−300 °C/s, depending on the current used. Such rapid heating allowed us to successfully synthesize sub-2 nm ultrasmall (US) CdSe QDs with only 2 s of heating. As shown in Figure 2, the absorption spectrum indicates that the particles have a narrow size distribution with an average diameter of 1.8 nm (calculated).[21] Through numerous experiments, a 2 s minimum heating time is needed to produce

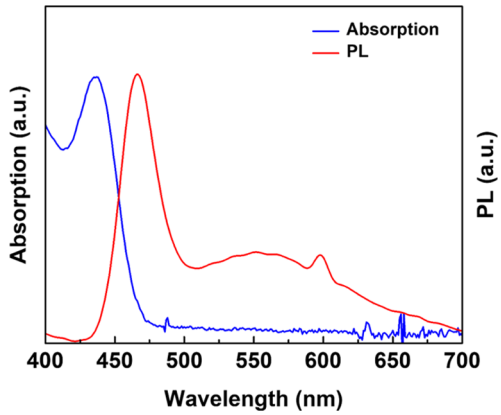


**Figure 2.** UV−vis absorption and PL spectra of CdSe QDs produced with IH. The absorption feature corresponds to a diameter of 1.8 nm.

particles with the present experimental apparatus. This is explained by the nonlinear relationship between heating rate and time caused by the increase of resistance in the steel balls as temperature rises. Therefore, it becomes increasingly less effective to increase heating rate by applying higher currents. In addition, the heat transfer rate between steel balls, solvent, and precursor molecules stays constant regardless of the current applied. At a certain point, it is not surprising that the heat transfer rate also becomes a bottleneck for achieving even faster synthesis. Even faster heating could be achieved with optimization of heat transfer so that particles can be produced with <2 s of heating, an unprecedented and greatly attractive prospect. Although heating is rapid, cooling is slow and particles continue to grow during the cooling process. Accelerated cooling can be implemented in our experimental setup and in a later section it will be shown that quenching has interesting effects on the different properties and characteristics of the particles produced. For potential scale-up, a flow-through setup can take advantage of this cooling as heated material can move through the heating chamber and continue to cool while new cold material moves in.

As a proof of concept, here, continuous synthesis of QDs is demonstrated with a modified flow-through setup. Figure 3 shows the setup and the absorption and photoluminescence (PL) spectra of two samples collected at different heating temperatures. The "high-heat" sample was collected at ∼250 °C, and the "low-heat" sample was collected at ∼150 °C. As expected, the low-heat sample showed overall smaller particle sizes, and the high-heat sample showed a mixture of small and larger sizes based on the absorption spectrum of the particles. In the present experiment, continuously running the synthesis at a roughly 1 mL/s pumping rate translates to just over 1 kg of nanoparticles produced per hour with a very crude estimation. In fact, a faster pumping rate would be more ideal as even the lowest heating current (2 A) is able to boil the solvent. Equilibrium of the heating temperature could be achieved by fine-tuning the pumping rate and heating current but requires more intricate engineering. Nevertheless, this demonstration of IH flow-through synthesis is compelling for scaling-up material production.

To show the novel properties and advantages of rapid IH synthesis, a set of data using CdSe has been obtained comparing IH, MW heating, and regular heat-up synthesis with a heating mantle, which typically runs at a heating rate of 1 °C/min (Figure 1). MW synthesis often obtains rapid heating



DOI: 10.1021/acsomega.8b00096
ACS Omega 2018, 3, 5399−5405

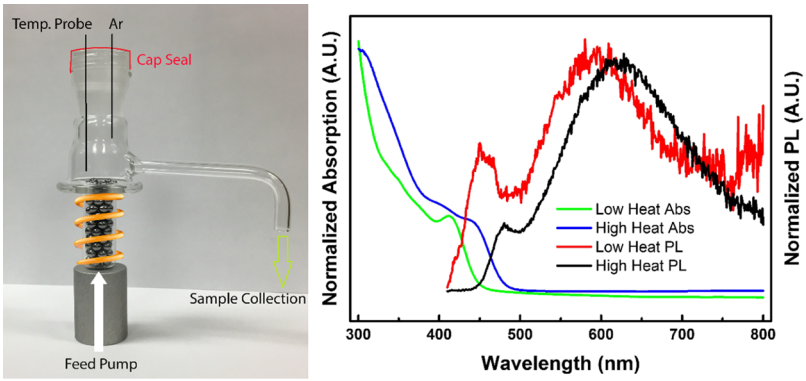


**Figure 3.** Left: Continuous synthesis setup; right: absorption and PL spectra of samples prepared at low (~150 °C) and high (~250 °C) temperatures using the continuous flow setup.

rates in comparison to traditional heat-up methods[15] but is also slower than IH (Figure 1). Nevertheless, MW heating provides a different heating mechanism for QD synthesis and therefore a different engineering control in industrial settings, so it will be compared with IH later. First, IH was compared with traditional heat-up synthesis using a heating mantle (normal heating). As shown in Figure 4, 2 s of IH produced an

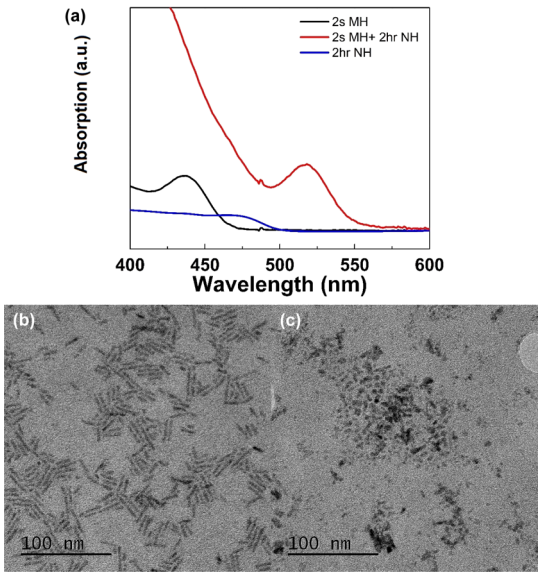


**Figure 4.** (a) Comparison of absorption spectra of CdSe QDs synthesized with 2 s of IH (2 s MH), 2 s of IH followed by 2 h of normal heating (2 s MH + 2 h NH), and 2 h of normal heating alone (2 h NH). TEM images of (b) 2 s MH + 2 h NH and (c) 2 h NH.

absorption peak centered at approximately 437 nm. After 2 h of normal heating, the absorption feature red-shifts. IH for 2 s followed by 2 h of normal heating resulted in a further red shift in the absorption peak. On the basis of the optical absorption of the particles, the growth kinetics have been altered significantly. The TEM images of the particles indicate very different shapes present in the growth solution. It can be clearly seen that the short IH induces the formation CdSe nanorods. We speculate that either the initial IH may produce more monodisperse US CdSe QDs followed by subsequent assembly to nanorods or the IH directly produces preferential growth in one direction of the CdSe QDs, resulting in the observed rod shape.

For comparison of IH to MW heating, the reaction conditions were made as similar as possible. The same precursor mixture was used, but only 2 mL per reaction to accommodate the 10 mL Pyrex vessel. In previous studies of MW-assisted QD synthesis, rapid heating was achieved by combining solvents that are not polar or ionic with good MW-absorbing precursors in a Pyrex vessel, so the MW radiation can interact directly with the molecules in the solution.[22] Reactions initially used a Pyrex vessel, but the reaction temperature failed to reach the set point of 200 °C as indicated by the temperature−time plot in the inset of Figure 5. This is likely

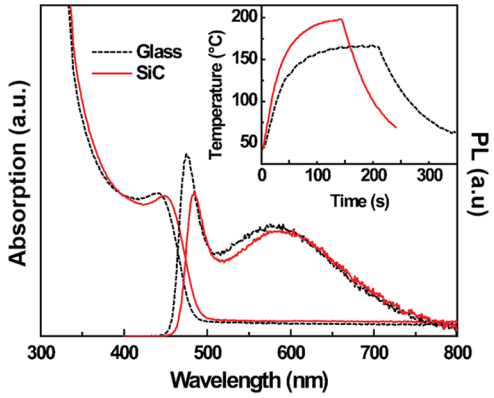


**Figure 5.** Absorption and PL spectra of US CdSe QDs synthesized using the SSP $Li_4[Cd_{10}Se_4(SPh)_{16}]$ in the MW reactor. The CdSe synthesis was carried out in both glass (black) and silicon carbide (SiC, red) vessels at a set temperature of 200 °C. The inset shows the corresponding temperature vs time plots and that the reaction failed to reach 200 °C in the glass vessel.

because the $Li_4Cd_{10}Se_4(SPh)_{16}$ cluster and DDA ligand are poor MW-absorbing materials.[23] However, using a SiC vessel, which absorbs most of the MW radiation, leads to convective heating that is similar to traditional heat-up methods, and the reaction reaches 200 °C (Figure 5, inset).[24] The UV−vis absorption and PL spectra of the CdSe QDs synthesized using the single-source precursor (SSP) in Pyrex and SiC vessels are shown in Figure 5. The red shift in both the absorption and emission peaks of the QDs prepared in the SiC vessel indicates a size increase of the CdSe QDs.

Although temperatures of 200 °C can be reached using the SiC vessel, to obtain the fastest heating rate using MW heating, a better MW absorbing material was used. Tri-*n*-octylphosphine (TOP) chalcogenides are established MW absorbers and can



DOI: 10.1021/acsomega.8b00096
*ACS Omega* 2018, 3, 5399−5405

lead to fast heating rates.[25] The reaction mixture contained $Cd(OA)_2$, TOPSe, and oleylamine (OLA). This mixture was heated to 150 °C at 850 W set power (SP) with hold times of 0, 15, and 30 s. The heating profile indicates that the heating rate is similar in all reactions, as seen in Figure 6 (inset) and the

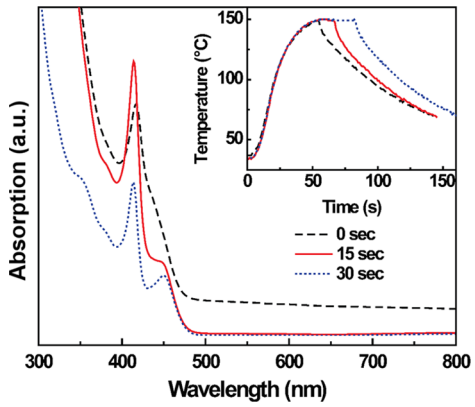


**Figure 6.** UV−vis absorption spectra of US CdSe QDs synthesized using $Cd(OA)_2$ and TOPSe in the MW reactor at 150 °C and 850 W SP with hold times of 0 (black), 15 (red), and 30 (blue) seconds. The inset shows the corresponding temperature vs time plots.

power versus time plots (Figure S3). As the hold time increases, the UV−vis absorption spectra show a slight red shift in the peak centered at 415 nm and a new peak appearing around 450 nm (Figure 6). The new peak at around 450 nm is a result of the size increase of the CdSe QDs from magic-size (MS) clusters to US QDs (diameters below 2 nm).[26] Dagtepe and Chikan have shown that having tellurium-rich (selenium in this study) conditions leads to the formation of MS QDs.[27] The systematic absorption peak shift shows that the CdSe size increases from MS to US following homogenous growth.[26] Figure 7 shows the PL and PL excitation (PLE) spectra for the

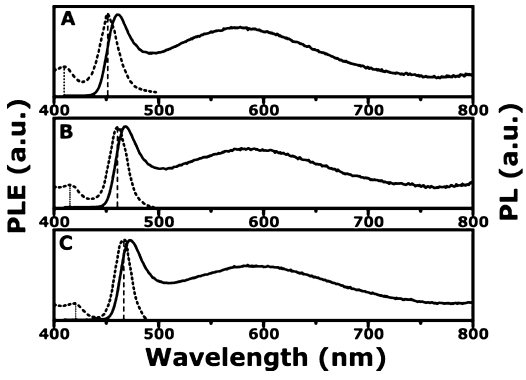


**Figure 7.** PL and PLE spectra of US CdSe QDs synthesized using $Cd(OA)_2$ and TOPSe in the MW reactor at 150 °C and 850 W SP with hold times of (A) 0, (B) 15, and (C) 30 s. The PL spectra were obtained using 405 nm excitation, and the PLE spectra were obtained for the emission at 575 nm.

US QDs. One of the unique properties of US QDs is the presence of two emission peaks: a higher energy band-edge peak and lower energy trap emission.[26] The sharp band-edge peak red-shifts from 460 nm (0 s) to 472 nm (30 s) as the hold time increases, but the emission profiles of small-sized QDs are dominated by trap emission because of their large surface-to-volume ratios.[28] Therefore, the second peak observed in the PL spectra is ascribed to the QDs instead of impurities in solution. To further investigate this, PLE spectra were recorded at different emission wavelengths. Figure 7 shows the excitation spectra with 575 nm detection. The similar features in the excitation spectra provide evidence that the second peak is trap emission from the QDs.

Because rapid MW-assisted heating was achieved with different precursors, we next compare CdSe QDs synthesized from the SSP and cadmium oleate (CdOA)−TOPSe mixture using IH. Figure 8 shows the absorption and PL spectra of the

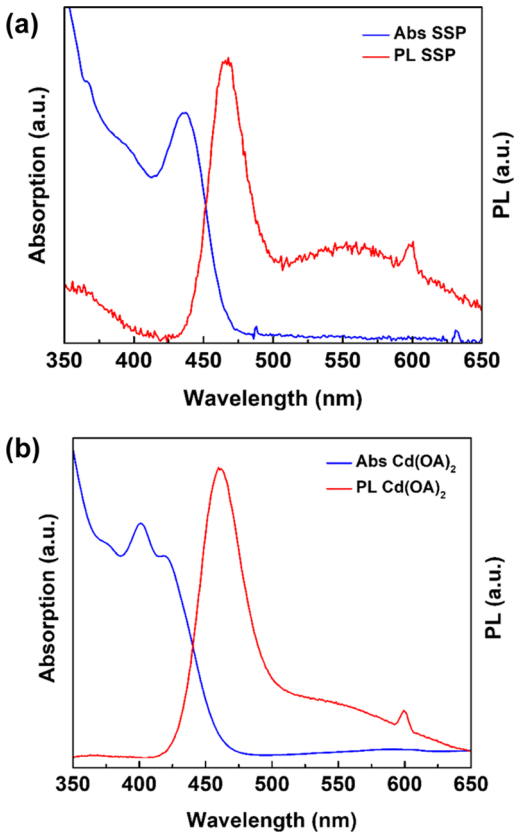


**Figure 8.** Comparison of absorption and PL spectra obtained from (a) the SSP $Li_4[Cd_{10}Se_4(SPh)_{16}]$ and (b) the mixed $Cd(OA)_2$−TOPSe precursor prepared with IH.

samples, and the shorter wavelength of the absorption peak corresponds to smaller particles produced with the mixed precursor compared to those formed from the SSP. A second peak corresponding to larger particles was also observed. The two distinct peaks are the result of the so-called sequential growth process, where distinct sizes of particles coexist at early stages of growth and then coalesce to form larger particles later.[29] Combined with the fact that the shorter peak wavelength corresponds to smaller particles produced than those from SSP, it is clear that the mixed precursor had a slower reaction rate than the SSP. Different reaction potentials of the precursor molecule can cause a difference in the nucleation rate, as it affects the rate at which monomers are provided. The mixed precursor provides monomers through combination of two components, whereas the SSP does so through self-decomposition of the precursor molecule, a process whose mechanism is not yet fully understood. Although it is difficult to determine the energies involved in either two reactions, we do



DOI: 10.1021/acsomega.8b00096
ACS Omega 2018, 3, 5399−5405

qualitatively show such an effect as an example of potential optimizations available for industrial applications.

Comparative syntheses of CdSe QDs in OLA and DDA were also performed. Previous studies suggest a correlation between the viscosity of solvent and the rate of nucleation, as it is related to the rate of diffusion of monomers.[30] Therefore, solvents with lower viscosity would result in higher nucleation rates and narrower size distributions. PL data (Figure S2) show no significant difference between samples prepared in solvents with different viscosities. Such a theory is made under the assumption of normal heating and stirring conditions, but with rapid IH, the effects of solvent viscosity and stirring become negligible. The nucleation process, which normally lasts several tens of minutes, is done in 2 s, and along with the fast self-stirring of solvent caused by thermal diffusion and degasification, differences caused by viscosity and stirring become less relevant. The slightly larger size of the particles prepared in DDA is explained by the higher solvent heat capacity, which kept the reaction mixture at a higher temperature, allowing the particles to grow for several minutes longer. Additionally, the lower trap-state emission intensity agrees with the slower cooling rate, as explained in the quenching section. Different ligand−particle structures with unknown electronic properties formed by the two solvents could also contribute to different levels of trap-state emission. This result revealed an unusual effect of extremely high heating rate not predicted under current theories. Future work will use appropriate modification to properly model the kinetics of nucleation and growth under such conditions.

Although fast heating rates can be achieved using MW-assisted synthesis, there are some limitations. Comparison of the SSP and mixed precursors shows that in the absence of a good MW absorber, rapid heating does not occur and the reaction temperature may not even be accessible. Another heating rate issue is illustrated in Figure S3. The power the instrument applies toward heating the reactions is not the reaction SP. This prevents arcing and overheating, which can lead to reaction vessel explosion because of pressure build-up. In Figure S3, although the reaction SP was 850 W, the power maximum was only around 450 W. As this is an instrument-specific issue, modification of the MW reactor to apply the SP could provide faster heating rates. Additional reaction modification such as the use of unreactive, excellent MW-absorbing materials (such as ionic liquids) can help achieve faster heating as well.[31] These are a few of the multiple conditions, not optimized here, available for reaching the fastest MW heating rates.

The preliminary IH syntheses explored the various effects of high heating rate from a thermodynamics point of view and are not optimized. Optimizations for the smallest particle size, shortest reaction time, control of PL, or other light-emitting functions are all desirable. All samples produced in these experiments exhibit both trap state and band edge state emissions, which is expected for small-sized particles with a high surface-to-volume ratio. A possible scenario is that the CdSe has emissive deep trap sites (Se vacancies) with the interaction of amine used as a solvent.[32] Giansante and Infante have shown that these surface traps could be potentially healed once the origin of the traps is identified unambiguously.[33] Our observation indicates that the emission quantum yield of the IH synthesis-produced QDs is less than 10%. The role of IH synthesis in the formation of defects (surface or otherwise) will be further investigated in a future publication.

## CONCLUSIONS

This study introduces a new IH method for CdSe synthesis and demonstrates the effects of extreme high heating rate on the growth kinetics of CdSe QDs. It is shown here that IH provides an effective means of reducing the nucleation stage window, resulting in greater control of particle size and size distribution. The results were compared with those of MW heating, which is an attractive rapid heating method in QD synthesis for its fine control of heating rate and rather uniform heating, so small changes in reaction conditions can be used to fine-tune QD properties reproducibly. Using MW-absorbing precursors provides faster heating and with these, both methods form US CdSe QDs in seconds without optimization. Preliminary demonstration of flow-through synthesis shows the potential of IH for rapid, large-scale production of QDs.

## EXPERIMENTAL SECTION

## MATERIALS

The following chemicals are used as received: cadmium nitrate tetrahydrate ($Cd(NO_3)_2{\cdot}4H_2O$, 99+%) from Acros Organics; thiophenol (PhSH, 97%), triethylamine (TEA, ≥99%), selenium powder (Se, ≥99.5%), OLA (≥98%), DDA (98%, degassed prior to use), indium acetate ($In(OAc)_3$, 99.99% trace metals basis), palmitic acid (≥99%), decane (≥99%), and 1-octadecene (90%), from Sigma-Aldrich; tri-*n*-octylphosphine (TOP) (97%), tris(trimethylsilyl)phosphine ($P(TMS)_3$, min. 98%, 10% in hexane), and indium acetate ($In(OAc)_3$, 99.99%) from Strem; lithium nitrate ($LiNO_3$, certified grade) and oleic acid (OA, ≥97%), from Fisher Scientific; and cadmium oxide (CdO, ≥99.0%) from Fluka. TOPSe (1 M) is prepared by mixing 10 mL of TOP with 0.7896 g of Se powder. The mixture is sonicated until all Se powder dissolves.

**$Li_4[Cd_{10}Se_4(SPh)_{16}]$ Precursor.** The $Li_4[Cd_{10}Se_4(SPh)_{16}]$ SSP is prepared as reported by Cumberland et al.[34] Briefly, at room temperature, $Li_2[Cd_4(SPh)_{10}]$ is first prepared by adding $Cd(NO_3)_2{\cdot}4H_2O$ in methanol to a solution of thiophenol and TEA in methanol, followed by addition of lithium nitrate in methanol. The mixture is then stirred and cooled to 0 °C to allow for crystallization. The washed and vacuum-dried precipitate is then dissolved in acetonitrile, followed by addition of selenium powder to produce $Li_4[Cd_{10}Se_4(SPh)_{16}]$. The precursor solution is prepared by adding 0.3 g of $Li_4[Cd_{10}Se_4(SPh)_{16}]$ to 25 mL of DDA.

**CdOA Precursor.** CdOA is prepared using CdO and OA at a 1:5 mole ratio as described previously.[35] The CdO powder and oleic acid are heated to 100 °C under vacuum in a round-bottom flask for 2 h. Then, the solution is put under $N_2$ and heated to 280 °C. The reaction is stopped after the color changes from red-brown to light yellow, in about an hour. On the basis of an adapted method,[25] the precursor solution is prepared by stirring a mixture of 0.675 g of CdOA, 5.5 mL of 1 M TOPSe, 10 mL of TOP, and 2 mL of OLA at 65 °C for 5 min in a 20 mL vial.

**QD Preparation by IH.** In a typical IH synthesis, the precursor and coordinating solvent (precursor solution) are mixed at 45 °C in a glass vessel fitted with an optical thermometer (Figure 1c). Steel beads (26.13 g, Bearing-Quality E52100 Alloy Steel, Hardened Ball, 1/8″ Diameter) are added, and the mixture is purged with argon for 5 min. Under argon flow, a current of 0−30.3 A is applied for various durations. The steel beads appeared unreactive toward the solution in the few



DOI: 10.1021/acsomega.8b00096
ACS Omega 2018, 3, 5399−5405

seconds (s) of heating applied. The temperature of the solution is lowered to 45 °C, and the sample is removed. The power output of the setup is estimated at >600 W while using highest current (20 A) and >100 W while using lowest current (2.5 A) by testing with IH of water.

For flow-through continuous synthesis, the abovementioned setup is modified as shown in Figure 3 (left). A thinner heating vessel with fewer steel balls provides better control of the heating rate. The precursor solution is preloaded into the pump tube and vessel, ensuring elimination of air bubbles. A pump connected by tube feeds the precursor solution into the heating vessel, so the flow rate and heating current can be adjusted on the fly during synthesis. Samples produced under these different parameters are collected.

**QD Preparation by MW Heating.** For MW syntheses, 2 mL samples are prepared in tightly capped 10G Anton Paar MW vessels with a stir bar. The synthesis is carried out in a MW reactor (Anton Paar Monowave 300) at 850 W (Figure 1b). The temperature is measured with an external IR probe. The MW method used the "heat-as-fast-as-possible" mode and a reaction time (holding time) of 0−60 s, followed by cooling to 55 °C using compressed air.

**Characterization of QDs.** UV−vis absorption spectra are recorded with a Cary 500 or a Cary 5000 UV−vis−NIR spectrophotometer. PL spectra are recorded using an Ocean Optics 2000+ spectrometer with 405 nm excitation and a PTI QuantaMaster 400 fluorometer, which is also used for PLE spectra. For absorption and emission spectra measurements, the samples are diluted in toluene to equal concentrations. In situ monitoring of temperature of MW syntheses is accomplished using an IR sensor. For transmission electron microscopy, the imaging is done on an FEI Tecnai G2 Spirit BioTWIN microscope. Samples are washed well in anhydrous methanol to remove excess ligands, dispersed in toluene, and dropped onto a Cu grid. The resolution of the instrument is 0.34 nm in the TEM mode.

## ■ ASSOCIATED CONTENT

### Supporting Information

The Supporting Information is available free of charge on the ACS Publications website at DOI: 10.1021/acsomega.8b00096.

TEM images of CdSe QDs synthesized using IH; PL spectra of CdSe QDs synthesized in amines; and power versus time plot for the MW-assisted synthesis of CdSe using the $Cd(OA)_2$ precursor (PDF)

## ■ AUTHOR INFORMATION


### Corresponding Authors

*E-mail: mclaurin@ksu.edu. Phone: 785-532-6528 (E.J.M.).
*E-mail: vchikan@ksu.edu. Phone: 785-532-6807 (V.C.).

### ORCID

Emily J. McLaurin: 0000-0002-7681-9587
Viktor Chikan: 0000-0002-4157-3556


### Notes

The authors declare no competing financial interest.

## ■ ACKNOWLEDGMENTS

The authors would like to acknowledge the Department of Chemistry at KSU for support and College of Veterinary Medicine for use of their TEM facility.

## ■ REFERENCES


(1) Nozik, A. J. Quantum Dot Solar Cells. *Phys. E* **2002**, *14*, 115−120.
(2) Carey, G. H.; Abdelhady, A. L.; Ning, Z.; Thon, S. M.; Bakr, O. M.; Sargent, E. H. Colloidal Quantum Dot Solar Cells. *Chem. Rev.* **2015**, *115*, 12732−12763.
(3) Atwater, H. A.; Polman, A. Plasmonics for Improved Photovoltaic Devices. *Nat. Mater.* **2010**, *9*, 205−213.
(4) Pankhurst, Q. A.; Thanh, N. T. K.; Jones, S. K.; Dobson, J. Progress in Applications of Magnetic Nanoparticles in Biomedicine. *J. Phys. D: Appl. Phys.* **2009**, *42*, 224001.
(5) Smith, B. R.; Gambhir, S. S. Nanomaterials for in Vivo Imaging. *Chem. Rev.* **2017**, *117*, 901−986.
(6) Narayanan, R.; El-Sayed, M. A. Catalysis with Transition Metal Nanoparticles in Colloidal Solution: Nanoparticle Shape Dependence and Stability. *J. Phys. Chem. B* **2005**, *109*, 12663−12676.
(7) Astruc, D.; Lu, F.; Aranzaes, J. R. Nanoparticles as Recyclable Catalysts: The Frontier between Homogeneous and Heterogeneous Catalysis. *Angew. Chem., Int. Ed.* **2005**, *44*, 7852−7872.
(8) Varma, R. S. Greener Routes to Organics and Nanomaterials: Sustainable Applications of Nanocatalysts. *Pure Appl. Chem.* **2013**, *85*, 1703−1710.
(9) Zhou, Z.-Y.; Tian, N.; Li, J.-T.; Broadwell, I.; Sun, S.-G. Nanomaterials of High Surface Energy with Exceptional Properties in Catalysis and Energy Storage. *Chem. Soc. Rev.* **2011**, *40*, 4167−4185.
(10) Hyeon, T. Chemical Synthesis of Magnetic Nanoparticles. *Chem. Commun.* **2003**, 927−934.
(11) Murray, C. B.; Kagan, C. R.; Bawendi, M. G. Synthesis and Characterization of Monodisperse Nanocrystals and Close-Packed Nanocrystal Assemblies. *Annu. Rev. Mater. Sci.* **2000**, *30*, 545−610.
(12) van Embden, J.; Chesman, A. S. R.; Jasieniak, J. J. The Heat-up Synthesis of Colloidal Nanocrystals. *Chem. Mater.* **2015**, *27*, 2246−2285.
(13) Kwon, S. G.; Hyeon, T. Formation Mechanisms of Uniform Nanocrystals Via Hot-Injection and Heat-up Methods. *Small* **2011**, *7*, 2685−2702.
(14) Thanh, N. T. K.; Maclean, N.; Mahiddine, S. Mechanisms of Nucleation and Growth of Nanoparticles in Solution. *Chem. Rev.* **2014**, *114*, 7610−7630.
(15) Jacob, J.; Chia, L. H. L.; Boey, F. Y. C. Thermal and Non-Thermal Interaction of Microwave Radiation with Materials. *J. Mater. Sci.* **1995**, *30*, 5321−5327.
(16) Kupracz, L.; Kirschning, A. Multiple Organolithium Generation in the Continuous Flow Synthesis of Amitriptyline. *Adv. Synth. Catal.* **2013**, *355*, 3375−3380.
(17) Gabriel, C.; Gabriel, S.; Grant, E. H.; Halstead, B. S. J.; Mingos, D. M. P. Dielectric Parameters Relevant to Microwave Dielectric Heating. *Chem. Soc. Rev.* **1998**, *27*, 213−224.
(18) Bilecka, I.; Niederberger, M. Microwave Chemistry for Inorganic Nanomaterials Synthesis. *Nanoscale* **2010**, *2*, 1358−1374.
(19) Zhu, Y.-J.; Chen, F. Microwave-Assisted Preparation of Inorganic Nanostructures in Liquid Phase. *Chem. Rev.* **2014**, *114*, 6462−6555.
(20) Chikan, V.; McLaurin, E. J. Rapid Nanoparticle Synthesis by Magnetic and Microwave Heating. *Nanomaterials* **2016**, *6*, 85.
(21) Jasieniak, J.; Smith, L.; van Embden, J.; Mulvaney, P.; Califano, M. Re-Examination of the Size-Dependent Absorption Properties of Cdse Quantum Dots. *J. Phys. Chem. C* **2009**, *113*, 19468−19474.
(22) Washington, A. L.; Strouse, G. F. Selective Microwave Absorption by Trioctyl Phosphine Selenide: Does It Play a Role in Producing Multiple Sized Quantum Dots in a Single Reaction? *Chem. Mater.* **2009**, *21*, 2770−2776.
(23) Gerbec, J. A.; Magana, D.; Washington, A.; Strouse, G. F. Microwave-Enhanced Reaction Rates for Nanoparticle Synthesis. *J. Am. Chem. Soc.* **2005**, *127*, 15791−15800.
(24) Ashley, B.; Lovingood, D. D.; Chiu, Y.-C.; Gao, H.; Owens, J.; Strouse, G. F. Specific Effects in Microwave Chemistry Explored through Reactor Vessel Design, Theory, and Spectroscopy. *Phys. Chem. Chem. Phys.* **2015**, *17*, 27317−27327.




DOI: 10.1021/acsomega.8b00096
*ACS Omega* 2018, 3, 5399−5405

(25) Washington, A. L., II; Strouse, G. F. Microwave Synthesis of CdSe and CdTe Nanocrystals in Nonabsorbing Alkanes. *J. Am. Chem. Soc.* **2008**, *130*, 8916−8922.
(26) Harrell, S. M.; McBride, J. R.; Rosenthal, S. J. Synthesis of Ultrasmall and Magic-Sized Cdse Nanocrystals. *Chem. Mater.* **2013**, *25*, 1199−1210.
(27) Dagtepe, P.; Chikan, V. Effect of Cd/Te Ratio on the Formation of CdTe Magic-Sized Quantum Dots During Aggregation. *J. Phys. Chem. A* **2008**, *112*, 9304−9311.
(28) McBride, J. R.; Dukes, A. D.; Schreuder, M. A.; Rosenthal, S. J. On Ultrasmall Nanocrystals. *Chem. Phys. Lett.* **2010**, *498*, 1−9.
(29) Kudera, S.; Zanella, M.; Giannini, C.; Rizzo, A.; Li, Y.; Gigli, G.; Cingolani, R.; Ciccarella, G.; Spahl, W.; Parak, W. J.; Manna, L. Sequential Growth of Magic-Size CdSe Nanocrystals. *Adv. Mater.* **2007**, *19*, 548−552.
(30) Kalwarczyk, T.; Sozanski, K.; Jakiela, S.; Wisniewska, A.; Kalwarczyk, E.; Kryszczuk, K.; Hou, S.; Holyst, R. Length-Scale Dependent Transport Properties of Colloidal and Protein Solutions for Prediction of Crystal Nucleation Rates. *Nanoscale* **2014**, *6*, 10340−10346.
(31) Zhu, Y.-J.; Wang, W.-W.; Qi, R.-J.; Hu, X.-L. Microwave-Assisted Synthesis of Single-Crystalline Tellurium Nanorods and Nanowires in Ionic Liquids. *Angew. Chem.* **2004**, *116*, 1434−1438.
(32) Baker, D. R.; Kamat, P. V. Tuning the Emission of CdSe Quantum Dots by Controlled Trap Enhancement. *Langmuir* **2010**, *26*, 11272−11276.
(33) Giansante, C.; Infante, I. Surface Traps in Colloidal Quantum Dots: A Combined Experimental and Theoretical Perspective. *J. Phys. Chem. Lett.* **2017**, *8*, 5209−5215.
(34) Cumberland, S. L.; Hanif, K. M.; Javier, A.; Khitrov, G. A.; Strouse, G. F.; Woessner, S. M.; Yun, C. S. Inorganic Clusters as Single-Source Precursors for Preparation of CdSe, ZnSe, and CdSe/ZnS Nanomaterials. *Chem. Mater.* **2002**, *14*, 1576−1584.
(35) Yu, W. W.; Peng, X. Formation of High-Quality CdS and Other II−VI Semiconductor Nanocrystals in Noncoordinating Solvents: Tunable Reactivity of Monomers. *Angew. Chem., Int. Ed.* **2002**, *41*, 2368−2371.



DOI: 10.1021/acsomega.8b00096
*ACS Omega* 2018, 3, 5399−5405